

Precarious ephemeral refugia during the earliest Triassic

Amanda Godbold¹, Shane Schoepfer¹, Shuzhong Shen², and Charles M. Henderson¹

¹Department of Geoscience, University of Calgary, Calgary, Alberta T2N 1N4, Canada

²State Key Laboratory of Palaeobiology and Stratigraphy, Nanjing Institute of Geology and Palaeontology, Chinese Academy of Sciences, Nanjing 210008, China

ABSTRACT

The term *refuge* describes, in both ecology and paleoecology, an ecosystem that acts as a sanctuary during times of environmental stress. This study tests the concept by examining the fate of a single community that lived ~50 k.y. after the end-Permian mass extinction (EPME). An assemblage of trace fossils, bivalves, and echinoids, living on a microbial mat in a slope environment, is preserved on a single bedding plane in the Shangsi section, south China. The microbial community was vital to the success of the refuge, acting as a stable substrate, food source, and oxygen supply. Shallow-water microbial communities have been interpreted as refugia, but this deeper site may have been critical to organisms with temperature sensitivities. Published paleotemperature calculations suggest sublethal surface temperatures of 34 °C at Shangsi. A species of cidaroid echinoid likely migrated to cooler deep waters to optimize development, suggesting that the success of this shallow-water clade is attributable to such refugia, when survival was most precarious after the EPME. The ecosystem was short lived, depending on low productivity and slow sedimentation. When conditions became suboptimal due to ash input and increasing productivity, the ecosystem quickly collapsed, allowing for colonization by opportunistic taxa including *Claraia* and microconchids. Elsewhere the ecosystem may have remained unchanged. Earliest Triassic refugia may have been restricted to these ephemeral environmental settings until organisms adapted to continuing harsh conditions.

INTRODUCTION

The end-Permian mass extinction (EPME) is the largest extinction event in Earth's history and marks the transition from the Paleozoic to the Modern evolutionary fauna. Although the overall cause continues to be a source of debate, the EPME is strongly associated with temperature change, ocean acidification, and anoxia (Shen and Bowring, 2014; Joachimski et al., 2012; Botjter et al., 2008; Wignall and Twitchett, 1996). This event serves as an important case study for the synergistic effects that these environmental stressors impose on marine ecosystems. The development of marine refugia is one of the consequences of these stressors.

The term *refuge* describes an ecosystem that acts as a sanctuary for organisms during times of environmental stress (Kauffman and Erwin, 1995). The traditional archetype for a marine refuge is an oceanic island with a small isolated ecosystem that contains a significant population of Lazarus taxa, which disappear from the fossil record before returning unchanged millions of years later. Numerous Early Triassic refugia or habitable zones have been described from various paleogeographic locations and depositional settings (Song et al., 2014; Forel et al., 2013; Beatty et al., 2008; Twitchett et al., 2004), but few were in deep water.

A bedding surface in the Shangsi section, south China (Fig. 1), provides a snapshot of an oligophotic upper slope seafloor with a

substantial echinoid population, deposited during the earliest Triassic (*Hindeodus parvus* zone). Full-body echinoid specimens are rare because echinoids exhibit poor preservation potential and nearly went extinct during the EPME (Twitchett and Oji, 2005). Our specimens, comparable to *Eotiaris* sp., were radially flattened with the aboral surface exposed, suggesting that they were buried rapidly and *in situ*. The discovery of these echinoids increases known species from the early Griesbachian to two (the other is *Miocidarid pakistanensis*; Kummel and Teichert, 1973).

Oxygen concentrations, temperature, and food availability are three important factors controlling modern echinoid distribution (Byrne et al., 2009). Geochemical redox proxies indicate suboxic conditions during deposition at Shangsi (Xiang et al., 2016), offering sufficient oxygen concentrations for echinoid survival. Paleotemperatures calculated from oxygen isotopes of conodont apatite at Shangsi indicate a rapid increase in surface temperatures to 34 °C (Joachimski et al., 2012; Chen et al., 2016), which would considerably impair the development of most modern echinoids (Byrne et al., 2009). Nearly all Early Triassic cidaroid echinoids are found within shallow marine deposits (Twitchett and Oji, 2005). We hypothesize that echinoids sought refuge within the cooler, deeper slope setting at Shangsi near the limits of the photic zone, where microbial mats acted as a stable substrate and sustainable food source,

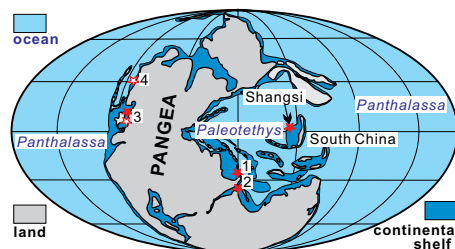


Figure 1. Paleogeographic map showing Shangsi (32.31926°N; 105.45440°E) section (China) and other localities. Closed red stars indicate Griesbachian echinoids; open stars are younger. 1—Wadi Wasit block, Oman (late Griesbachian); 2—Salt Range, Pakistan (early Griesbachian); 3—late Griesbachian Dinwoody Formation, Spathian Virgin Limestone Member, western United States; 4—Ladinian of north-east British Columbia, Canada.

allowing the seafloor to meet all basic environmental requirements of a refuge as predicted by Song et al. (2014). However, this ecosystem was short lived. We therefore explore the conditions that allowed for habitation within this refuge, and test the validity of the original refugia concept.

GEOLOGIC SETTING

The Shangsi section is located near Guangyuan, Sichuan Province, China. It was deposited at estimated water depths of 150–200 m, in an upper slope environment adjacent to a tropical or subtropical intracratonic platform on the south China microcontinent (Xiang et al., 2016), within the Paleotethys Ocean (Fig. 1). We investigated the upper 1.45 m of the upper Permian Talung Formation, a resistant, siliceous carbonaceous mudstone to wackestone. The base of our studied interval is a bedding plane in bed 22 at 98.7 m, with an abundant pelagic fauna dominated by ammonoids and nautiloids. We also investigated the lower 2.6 m of the Feixianguan Formation, composed primarily of recessive, yellow-green–weathering calcareous shale and argillaceous mudstone, as well as occasional ash beds and thin microbialite units. The formation contact is at 100.15 m, with the EPME at 100–100.2 m and the Permian-Triassic boundary (PTB) tentatively set in bed 28a at 100.3 m (Fig. 2A), although previous studies have suggested a higher level (Nicoll et al., 2002). The focus of this study is a bedding plane (top of

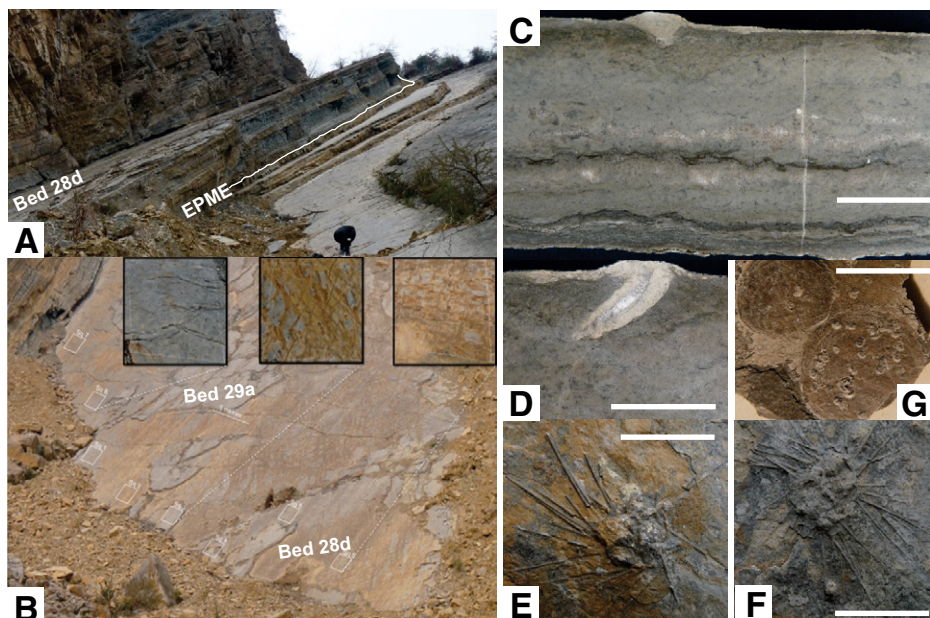


Figure 2. Outcrop, lithology, and fossils from study site in China (2 cm scale bar in C–G). A: Outcrop with position of end-Permian mass extinction (EPME), bed 28d surface and bed 29a. B: Mapped bedding plane with 1 m² quadrats. C: Microbialite laminae and fenestral fabric in upper bed 28d. D: *Cylindrichnus*? Cross section. E, F: Cidaroid echinoids from bed 28d. G: *Claraia wangi* from bed 29a; microconchids attached.

bed 28d) at 102.7 m within the *H. parvus* zone (see the Biostratigraphy section in the GSA Data Repository¹). This interpolates to ca. 251.89 Ma, ~10 k.y. into the Triassic and ~50 k.y. after the initial extinction, based on an age of 251.941 ± 0.037 Ma for the extinction (Burgess et al., 2014).

METHODS

Field Collection

The well-exposed bedding surface allowed us to employ the quadrat method (Fig. 2B), commonly used in modern ecologic studies, to determine organism abundance and distribution. Eight separate 1 m² quadrats were drawn directly on the bedding surface with chalk. Quadrats were spaced across ~80 m² surface of the bedding plane, at least 5 m apart to avoid bias. The number, position, and size of fossil taxa visible in each quadrat were recorded and photographed (Fig. 2B).

Geochemistry

Geochemical samples (n = 10) were analyzed for trace elements and stable isotopes. Trace elements were measured in powdered samples using a Niton XL3t handheld X-ray fluorescence analyzer. Organic carbon and nitrogen were analyzed on a Thermo Finnigan Delta V isotope

ratio mass spectrometer (IRMS) connected to an Elementar Cube elemental analyzer. Carbonate isotopes were determined on a Thermo Finnigan Delta V IRMS with Gasbench peripheral. Detailed laboratory methods and all data are reported in Table DR1 in the Data Repository.

RESULTS AND DISCUSSION

Unlike other paleontologic, geochronologic, and geochemical studies on the PTB interval at Shangsi (Riccardi et al., 2007; Jiang et al., 2011; Shen et al., 2011; Xiang et al., 2016), our work focused on a single bedding plane and the few immediately overlying centimeters of strata. In contrast to most paleoecologic studies, there is negligible time averaging in our bedding-plane sample, meaning that this ancient ecosystem is studied at an ecologic time scale. We describe a fossil-rich surface, and the geochemistry both below and above that surface, to understand environmental changes affecting this short-lived community. Such surfaces are likely common in lower Triassic rocks, but have either been missed or incorporated within larger trenched samples. We contend that such surfaces are vital to understanding earliest stages of recovery from Earth's greatest extinction.

Paleontology and Geochemistry of Echinoid-Dominated Bed

Bed 28d consists of a calcimicrobial limestone ~20 cm thick. The calcimicrobial mats show a wavy laminated texture separated by thin films of iron oxide-rich micrite. Ostracods, bivalves, and sponge spicules occur at low abundances within

the microbial mat. Euhedral pyrite occurs along the bed surface, penetrating the top few layers of microbial mats. Fossil taxa exposed along the upper surface of bed 28d (Fig. 2) include one cidaroid echinoid species, one ammonoid species, five bivalve species, and one type of domichnia trace fossil. The population density and distribution of these taxa show an average of one echinoid, one trace fossil, and eight bivalves per square meter (see the Data Repository). Only two ammonoids were found within the eight quadrats.

Although the diversity of taxa is low, the population density of cidaroid echinoids is high given the earliest Triassic age. The echinoids are restricted to this bedding plane at this site, suggesting the development of a simple, but effective, refuge. Microbial mats provided a firm substrate for echinoid grazing and are known to serve as a food source (Forel et al., 2013), meeting the minimal necessary conditions for a sustainable ecosystem.

The presence of microbial mats suggests that sufficient light reached the seafloor to support photosynthesis. Shangsi was likely at the limit or deeper than the normal base of the photic zone. However, light may have penetrated deep into the water column during the earliest Triassic, due to the regional collapse in marine productivity (Algeo et al., 2013; Shen et al., 2015) and associated decrease in turbidity. The generally low total organic carbon (TOC; <0.1%) and phosphorous (P; undetectable) contents suggest an extremely low productivity regime. The low nitrogen isotope values observed here (<0.5‰) and across south China (Luo et al., 2011) reflect a regime in which cyanobacterial N-fixers had an ecologic advantage, which may reflect nitrogen-limitation (Grasby et al., 2016).

The photosynthetic fractionation effect ($\Delta^{13}\text{C}$) observed in carbon isotopes from the echinoid bed is ~25‰ (Fig. DR6), lower than the typical value for marine photosynthesis. Our results are consistent with those of Riccardi et al. (2007), who interpreted these intervals as representing an ecologic contribution of phototrophic sulfur bacteria, in response to upward excursions of euxinic deep waters. However, other geochemical redox proxies (Mo and U; Fig. 3) indicate potential suboxia, but not euxinia in this interval. If the low $\Delta^{13}\text{C}$ observed in this bed indicates the presence of green sulfur bacteria, they may have lived as part of the seafloor microbial mat community rather than as plankton. Diagenetic pyrite indicates sulfide in the sediment pore water, and upward diffusion of sulfide to the sediment water interface may have provided green sulfur bacteria with sufficient reductant to survive even in an oxic to suboxic water column.

Paleontology and Geochemistry of the Overlying Bed

A number of geochemical indicators suggest that *Claraia* (Fig. 2G) proliferated in response

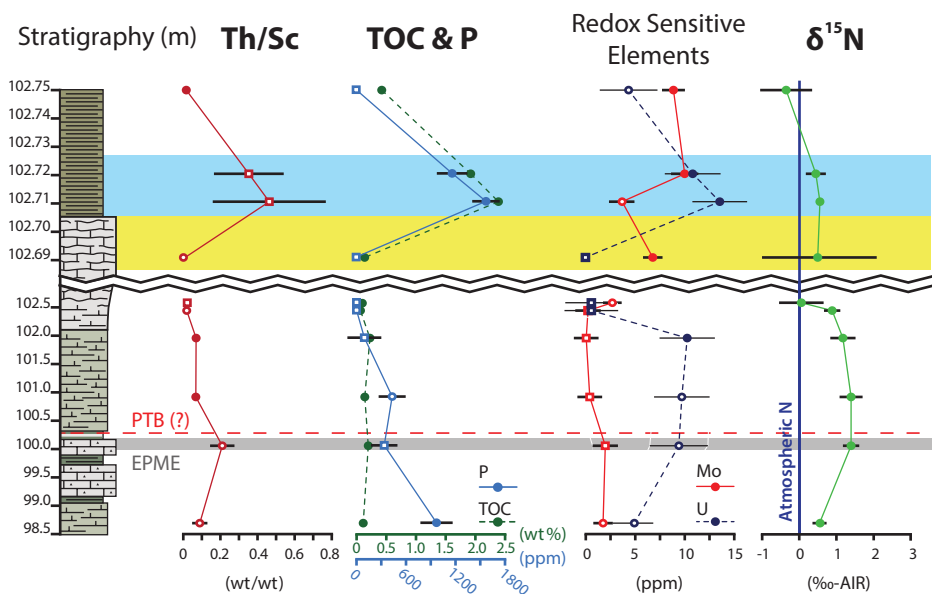


Figure 3. Stratigraphic trends in provenance, productivity, and redox proxies. TOC—total organic carbon; EPME—end-Permian mass extinction; PTB—Permian-Triassic boundary. Filled circles indicate all triplicate X-ray fluorescence measurements above the automated limit of detection (LOD) threshold; hollow circles indicate some measurements >LOD; hollow squares indicate all measurements <LOD. Yellow highlighted interval is the echinoid-dominated assemblage (bed 28d). Blue highlighted interval corresponds to the *Claraia*-dominated assemblage (bed 29a). Note the expanded scale above 102.5 m.

to a sudden ecologic disturbance. The ratio of thorium to scandium (Fig. 3), an indicator of provenance in marine sediments, becomes rapidly elevated, suggesting a sudden influx of more felsic material. Because this transition appears sudden rather than gradual, it likely reflects a rhyolitic ash fall. In addition to triggering an influx of terrestrial clastic material, this ash fall may have stimulated marine productivity, as has been observed elsewhere in south China (Shen et al., 2012). TOC is elevated in this horizon, with two samples yielding values of >1.5% TOC. This is significantly higher than the carbon content seen elsewhere in the section, including the latest pre-extinction Permian (Xiang et al., 2016). Small enrichments in Mo and U (Fig. 3; <12 ppm) suggest that bottom-water conditions may have been slightly more reducing in this interval and P content increases to values >1000 ppm. Phosphorous exhibits less preservation potential under reducing conditions, so this positive correlation suggests that elevated P and TOC values reflect high primary productivity (Schoepfer et al., 2015).

The calculated photosynthetic fractionation effect ($\Delta^{13}\text{C}$) increases by 4‰, which may reflect the development of a productivity regime dominated by a more normal community of aerobic and photosynthetic phytoplankton in the water column, rather than sulfide-oxidizing or partially chemosynthetic microbial mats. Increased water-column productivity and clastic input would have the combined effect of increasing turbidity and shading-out benthic photosynthesizers at upper slope water depths, while promoting a

community dominated by epibenthic suspension feeders (e.g., *Claraia*).

CONCLUSIONS

Refugia during the Permian-Triassic extinction have often been envisioned as oases of biodiversity that escaped the worst effects of the end-Permian event, or persisted in a narrow habitable zone or refuge within the otherwise lethal Early Triassic world (Twitchett et al., 2004; Beatty et al., 2008; Song et al., 2014). This model does

not seem to apply to Shangsi, where the environment allowed for the immediate short-term survival of echinoids and other biota during the first ~50 k.y. after extinction, but underwent a rapid, catastrophic disruption, while remaining in the refuge zone (*sensu* Song et al., 2014). This stress appears to have been temporary and local to regional in extent, in the form of a volcanic eruption and associated turbidity. The assemblage failed to recover, and was instead replaced by a depauperate assemblage of opportunistic taxa (Fig. 4B).

If the earliest Triassic world is envisioned as a shifting patchwork of temporary refugia, then the ability to migrate or disperse over wide areas would increase the probability of survival in a favorable environment. Migration must be envisioned in both the horizontal and vertical dimensions, with an organism's tolerance for low-light and high-pressure conditions allowing it to respond to surface temperature stress by moving into deeper water. While modern planktic echinoid larvae generally act as passive particles, it has been suggested that they may be able to alter their vertical distribution in response to different environmental cues such as surface temperature, food availability, and predation (Burdett-Coutts and Metaxas, 2004). The thermal tolerance of modern subtropical and tropical planktic echinoid larvae varies from the mid-20s °C to mid-30s °C (Song et al., 2014). While surface temperatures were in the mid-30s °C (Joachimski et al., 2012), modeling results for the earliest Triassic Paleotethys Ocean suggest that temperatures at 150–200 m water depth may have been 5–10 °C cooler than the surface ocean (Winguth et al., 2015). Echinoids likely colonized the bed 28d surface via the dispersal of resilient planktic larvae, with

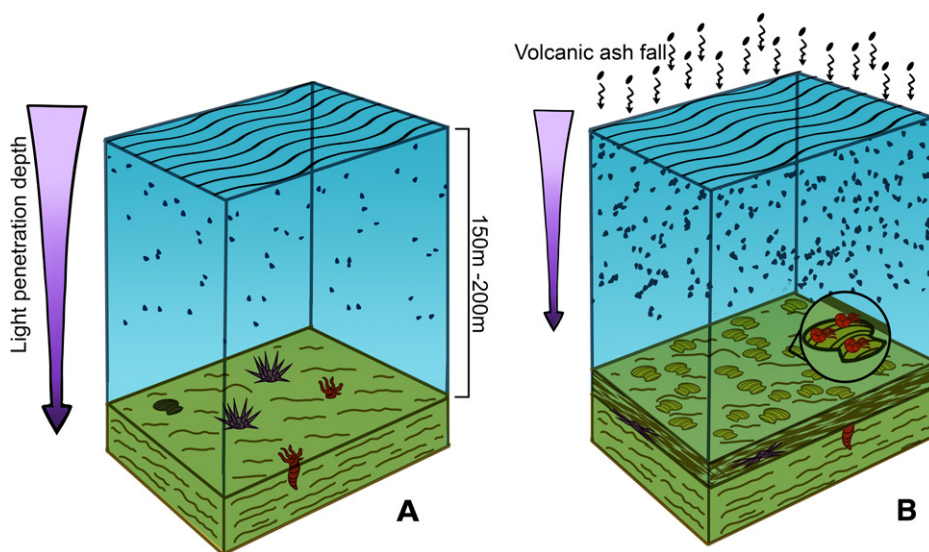


Figure 4. Schematic model. A: Bed 28d (the echinoid-dominated assemblage with low productivity and clear water). B: Bed 29a (*Claraia*-dominated assemblage, ash and high-productivity shade community).

those settling in cooler water sites having more optimal conditions for development.

Echinoid material is rare in the Griesbachian and more common by the Spathian (Schubert and Bottjer, 1995). Individual echinoid spines have been found in wackestone in the upper Griesbachian Dinwoody Formation of western North America (Rodland and Bottjer, 2001), suggesting an environment below wave base. Echinoids are also known from the eastern Tethys, including the shallow-water Wadi Wasit block in Oman (Fig. 1), with a diverse fauna (Twitchett et al., 2004) including echinoid spines during the late Griesbachian (*Isarcicella isarcica* Zone). This suggests, either that temperature stress was not the only factor limiting the distribution of echinoids, or that equatorial echinoid populations adapted during the *H. parvus* Zone to the point where temperature no longer was a limiting factor. The only other known early Griesbachian cidaroid, from the Salt Range of Pakistan, occurs in association with holdover Permian taxa (Kummel and Teichert, 1973) at a higher latitude where surface temperatures would be cooler (Fig. 1).

Our results demonstrate that species were able to precariously cling to life in ephemeral refugia immediately following the EPME. Such ephemeral refugia may have been the characteristic environments in which marine life initially recovered from Earth's greatest extinction, challenging the concept of refugia as isolated, long-lived, and undiscovered oases of biodiversity.

ACKNOWLEDGMENTS

This research was supported by the National Science Foundation of China (NSFC) (41290206) and the Strategic Priority Research Program (B) of the Chinese Academy of Sciences (XDB18000000) to Shen and by a Natural Sciences and Engineering Research Council of Canada (NSERC) Discovery Grant to Henderson. We thank Alisa Romanova for drafting Figure 4, and Sam Bowring for bringing this study site to our attention; he was the first to recognize the significance of this surface. Helpful reviews by Haishui Jiang, Margaret Fraiser, and an anonymous reviewer improved this manuscript.

REFERENCES CITED

Algeo, T.J., Henderson, C.M., Tong, J.N., Feng, Q.L., Yin, H.F., and Tyson, R.V., 2013, Plankton and productivity during the Permian-Triassic boundary crisis: An analysis of organic carbon fluxes: *Global and Planetary Change*, v. 105, p. 52–67, doi:10.1016/j.gloplacha.2012.02.008.

Beatty, T.W., Zonneveld, J.P., and Henderson, C.M., 2008, Anomalously diverse Early Triassic ichnofossil assemblages in northwest Pangea: A case for a shallow-marine habitable zone: *Geology*, v. 36, p. 771–774, doi:10.1130/G24952A.1.

Bottjer, D.J., Clapham, M.E., Fraiser, M.L., and Powers, C.M., 2008, Understanding mechanisms for the end-Permian mass extinction and the protracted

Early Triassic aftermath and recovery: *GSA Today*, v. 18, p. 4–10, doi:10.1130/GSATG8A.1.

Burdett-Coutts, V., and Metaxas, A., 2004, The effect of the quality of food patches on larval vertical distribution of the sea urchins *Lytechinus variegatus* (Lamarck) and *Strongylocentrotus droebachiensis* (Mueller): *Journal of Experimental Marine Biology and Ecology*, v. 308, p. 221–236, doi:10.1016/j.jembe.2004.02.023.

Burgess, S.D., Bowring, S., and Shen, S.Z., 2014, High-precision timeline for Earth's most severe extinction: *National Academy of Sciences Proceedings*, v. 111, p. 3316–3321, doi:10.1073/pnas.1317692111.

Byrne, M., Ho, M., Selvakumaraswamy, P., Nguyen, H.D., Dworjany, S.A., and Davis, A.R., 2009, Temperature, but not pH, compromises sea urchin fertilization and early development under near-future climate change scenarios: *Royal Society of London Proceedings*, ser. B, v. 276, p. 1883–1888, doi:10.1098/rspb.2008.1935.

Chen, J., et al., 2016, High-resolution SIMS oxygen isotope analysis on conodont apatite from south China and implications for the end-Permian mass extinction: *Palaeogeography, Palaeoclimatology, Palaeoecology*, v. 448, p. 26–38, doi:10.1016/j.palaeo.2015.11.025.

Forel, M.B., Crasquin, S., Kershaw, S., and Collin, P.Y., 2013, In the aftermath of the end-Permian extinction: The microbialite refuge: *Terra Nova*, v. 25, p. 137–143, doi:10.1111/ter.12017.

Grasby, S.E., Beauchamp, B., and Knies, J., 2016, Early Triassic productivity crises delayed recovery from world's worst mass extinction: *Geology*, v. 44, p. 779–782, doi:10.1130/G38141.1.

Jiang, H.S., Lai, X.L., Yan, C.B., Aldridge, R.J., Wignall, P.W., and Sun, Y.D., 2011, Revised conodont zonation and conodont evolution across the Permian-Triassic boundary at the Shangsi section, Guangyuan, Sichuan, south China: *Global and Planetary Change*, v. 77, p. 103–115, doi:10.1016/j.gloplacha.2011.04.003.

Joachimski, M.M., Lai, X.L., Shen, S.Z., Jiang, H., Luo, G., Chen, B., Chen, J., and Sun, Y., 2012, Climate warming in the latest Permian and the Permian-Triassic mass extinction: *Geology*, v. 40, p. 195–198, doi:10.1130/G32707.1.

Kauffman, E.G., and Erwin, D.H., 1995, Surviving mass extinctions: *Geotimes*, v. 40, p. 14–17.

Kummel, B., and Teichert, C., 1973, The Permian-Triassic boundary beds in central Tethys, in Logan, A., and Hills, L.V., eds., *The Permian Triassic systems and their mutual boundary*: Canadian Society of Petroleum Geologists Memoir 2, p. 17–34.

Luo, G., Wang, Y., Algeo, T.J., Kump, L.R., Bai, X., Yang, H., Yao, L., and Xie, S., 2011, Enhanced nitrogen fixation in the immediate aftermath of the latest Permian marine mass extinction: *Geology*, v. 39, p. 647–650, doi:10.1130/G32024.1.

Nicoll, R.S., Metcalfe, I., and Cheng-Yuan, W., 2002, New species of the conodont Genus *Hindeodus* and the conodont biostratigraphy of the Permian-Triassic boundary interval: *Journal of Asian Earth Sciences*, v. 20, p. 609–631, doi:10.1016/S1367-9120(02)00021-4.

Riccardi, A., Kump, L.R., Arthur, M.A., and D'Hondt, S., 2007, Carbon isotopic evidence for chemocline upward excursions during the end-Permian event: *Palaeogeography, Palaeoclimatology, Palaeoecology*, v. 248, p. 73–81, doi:10.1016/j.palaeo.2006.11.010.

Rodland, D.L., and Bottjer, D.J., 2001, Biotic recovery from the end-Permian mass extinction: Behavior of the inarticulate brachiopod *Lingula* as a disaster taxon: *Palaios*, v. 16, p. 95–101, doi:10.1669/0883-1351(2001)016<0095:BRFTEP>2.0.CO;2.

Schoepfer, S.D., Shen, J., Wei, H., Tyson, R.V., Ingall, E., and Algeo, T.J., 2015, Total organic carbon, organic phosphorus, and biogenic barium fluxes as proxies for paleomarine productivity: *Earth-Science Reviews*, v. 149, p. 23–52, doi:10.1016/j.earscirev.2014.08.017.

Schubert, J.K., and Bottjer, D.J., 1995, Aftermath of the Permian-Triassic mass extinction event: Paleogeology of Lower Triassic carbonates in the western USA: *Palaeogeography, Palaeoclimatology, Palaeoecology*, v. 116, p. 1–39, doi:10.1016/0031-0182(94)00093-N.

Shen, J., Algeo, T.J., Hu, Q., Zhang, N., Zhou, L., Xia, W., Xie, S., and Feng, Q., 2012, Negative C-isotope excursions at the Permian-Triassic boundary linked to volcanism: *Geology*, v. 40, p. 963–966, doi:10.1130/G33329.1.

Shen, J., Schoepfer, S.D., Feng, Q.L., Zhou, L., Yu, J.X., Song, H.Y., Wei, H.Y., and Algeo, T.J., 2015, Marine productivity changes during the end-Permian crisis and Early Triassic recovery: *Earth-Science Reviews*, v. 149, p. 136–162, doi:10.1016/j.earscirev.2014.11.002.

Shen, S.Z., and Bowring, S.A., 2014, The end-Permian mass extinction: A still unexplained catastrophe: *National Science Review*, v. 1, p. 492–495, doi:10.1093/nsr/nwu047.

Shen, S.Z., et al., 2011, Calibrating the End-Permian mass extinction: *Science*, v. 334, p. 1367–1372, doi:10.1126/science.1213454.

Song, H., Wignall, P.B., Chu, D., Tong, J., Sun, Y., Song, H., He, W., and Tian, L., 2014, Anoxia/high temperature double whammy during the Permian-Triassic marine crisis and its aftermath: *Scientific Reports*, v. 4, p. 1–7, doi:10.1038/srep04132.

Twitchett, R.J., and Oji, T., 2005, Early Triassic recovery of echinoderms: *Comptes Rendus Palévol*, v. 4, p. 531–542, doi:10.1016/j.crpv.2005.02.006.

Twitchett, R.J., Krystyn, L., Baud, A., Wheeler, J.R., and Richoz, S., 2004, Rapid marine recovery after the end-Permian mass-extinction event in the absence of marine anoxia: *Geology*, v. 32, p. 805–808, doi:10.1130/G20585.1.

Wignall, P.B., and Twitchett, R.J., 1996, Oceanic anoxia and the end Permian mass extinction: *Science*, v. 272, p. 1155–1158, doi:10.1126/science.272.5265.1155.

Winguth, A.M., Shields, C.A., and Winguth, C., 2015, Transition into a hothouse world at the Permian-Triassic boundary—A model study: *Palaeogeography, Palaeoclimatology, Palaeoecology*, v. 440, p. 316–327, doi:10.1016/j.palaeo.2015.09.008.

Xiang, L., Schoepfer, S.D., Zhang, H., Yuan, D.X., Cao, C.Q., Zheng, Q.F., Henderson, C.M., and Shen, S.Z., 2016, Oceanic redox evolution across the end-Permian mass extinction at Shangsi, south China: *Palaeogeography, Palaeoclimatology, Palaeoecology*, v. 448, p. 59–71, doi:10.1016/j.palaeo.2015.10.046.

Manuscript received 11 November 2016
Revised manuscript received 9 March 2017
Manuscript accepted 9 March 2017

Printed in USA